Egypt. J. Chem. **Vol. 61**, No.2, pp. 361 - 378 (2018)

Synthesis [1-(4-acetylphenyl)-3-(2-methylphenyl)]triazene: NMR, Vibrational, X-ray Crystallography Characterization with HF/ DFT Studies

Reza Soleymani[1*], Abolfazl Aghaei[2], Elahe Abdolahi Shahvali[3]

[1]*Young Researchers and Elite Club, Shahr-E-Rey Branch, Islamic Azad University, Tehran, Iran.*

[2]*Faculty of Chemistry, Tarbiat Moallem University, Tehran, Iran.*

[3]*Department of Chemistry, Dezful Branch, Islamic Azad University, Dezful, Iran.*

[1-(4-acetylphenyl)-3-(2-methylphenyl)]triazene (AMT) was synthesized by experimental methods, its chemical and spectrometric properties were studied by FT-IR, FT-Raman,^{1}H-NMR,^{13}C-NMR and X-ray single-crystal diffraction methods. The obtained results showed that this structure has orthorombic system with space group of pbca and eight molecules in unit cell. Its unit cell parameters comprise a=8.0665(2), b=8.0019(2) and c=21.5249(5). Then molecular number of [1-(4-acetylphenyl)-3-(2-methylphenyl)]triazene (AMT) structure has been studied by HF/DFT methods. However, FT-IR, FT-Raman,^{1}H-NMR, ^{13}C-NMR spectra were analyzed that the obtained results for vibrational spectra and amount of chemical shift correspond significantly with theoretical methods. Some structural parameters such as bonds length, bonds angle and dihedral angle were studied using theoretical and experimental methods. The parameters such as thermodynamical parameters, dipole moment, HOMO and LUMO energetic values, electrophilicity (ω), chemical potential(μ), chemical hardness(η) and max amount of electronic charge transfer (ΔN_{max}) are calculated for this compound in conclusion. The proposed methods were successfully applied to the determination of vibrational spectra, chemical shift amounts and structural parameters.

Keywords: Triazene, Crystal structure, Vibrational frequency, NMR.

Introduction

Triazenes are a group of compounds with diazo amino functional group and they have high stability to photo, thermo and acids [1-7]. They commonly adopt a trans configuration in the ground state [8]. Triazene compounds contain intramolecular charge-transfer chromophores and, therefore, the presence of electron donating and -withdrawing moieties will have appreciable effect on their UV–vis absorption bands [9-11]. Triazene compounds have been used for the preparation of several sensors for determination of heavy metals [12, 13], and also used in solid-phase extraction [14, 15]. They have been studied for their anorectic activity and potency against specific tumor cell lines [16–20], as well as they have been applied as protecting groups in natural product synthesis [21, 22] or used to form heterocycles [23, 24]. Various compounds have been prepared from these compounds, because of linkage ability of them to carbonic nano tubes that have important abilities especially in man's body metabolism [25]. A kind of these compounds applied in agronomy chemistry for insecticides and weeds synthesis [26, 27]. However, they have been used in pigments synthesis [27]. Recently, these compounds have been used as ligand to complex synthesis because they have many applications and abilities [11, 28-33]. In some of the triazene complexes variance in molecular structure and present creation possibility of attractive molecular interactions, causes to sit these compounds in super molecules family. The super molecules can use from covalent slender and reversible interaction such as Van der Waals power or hydrogen bond for molecules collection which causes to engender the new properties catalytic activity, new magnetic characterization and response to photo and the structure is applied in many new tendencies [34-36]. This inorganic compounds series can possess special properties and high application, [1-(4-acetylphenyl)-3-(2-methylphenyl)]triazene (AMT) can be synthesized by many studies and consideration as

*Corresponding author e-mail: reza.soleymani@hotmail.com
Tel: +98 2633350468- Mob: +98 9123782899

DOI: 10.21608/ejchem.2018.2176.1173

©2017 National Information and Documentation Center (NIDOC)

a new type of triazene compound. Its properties were performed some spectroscopic and thermodynamics studies for further consideration. Thus, FT-IR, FT-Raman, ^{1}H-NMR, ^{13}C-NMR and X-ray single crystal diffraction were studied. Then, this structure in levels HF and DFT were calculated theatrically and the theoretical results of IR vibrational spectra were analyzed Potential Energy Distributions (PEDs) computation and the obtained was compared with experimental results. However, thermodynamic parameters and electrophilicity value, chemical hardness, chemical potential and max amount of electronic charge transfer were calculated via the HOMO and LUMO energetic values.

The electrophilicity index, which measures the stabilization in energy when the system acquires an additional electronic charge, ΔN from the environment and is presented in terms of the electronic chemical potential, μ (the negative of electronegativity, χ) and the chemical hardness, η. Both quantities may be approximated in terms of the energies of frontier molecular orbitals ($\varepsilon_{HOMO}$and ε_{LUMO}) as $\mu = (\varepsilon_H+\varepsilon_L)/2$ and $\eta=\varepsilon_L-\varepsilon_H$. The Electrophilicity can also be approximated in terms of the ionization potential (I) and electron affinity (A) [37]. High values of μ and low values of η, characterize a good electrophone species. The maximum amount of electronic charge ΔN_{max}, that the electrophone system may accept [37, 38]. While the quantity of ω describes the propensity of the system to acquire additional electronic charge from the environment, the quantity of ΔN_{max} describes the charge capacity of molecule [37].

Experimental

General method

All materials were obtained from Sigma-Aldrich and were used without further purification. The Perkin Elmer RXI spectrometer was used to obtain IR spectra and using KBr disks in the frequency range of 4000-400 cm^{-1}. The Almega Thermo Nicolet Dispersive Raman spectrometer was used to obtain Raman spectra in the frequency range of 4200-100 cm^{-1}. Elemental analysis was carried out using a Perkin–Elmer 2400(II) CHNS/O analyzer. Melting points were measured on a Barnstead Electrothermal 9200 apparatus. The solution absorbencies were monitored using Perkin-Elmer Lambda 25 spectrophotometer, using two matched 10 mm quartz cells. ^{1}H NMR and ^{13}C NMR spectra were recorded on Bruker Avance 300 MHz spectrometer in deuterated dimethylsulfoxide (DMSO-d_6) solvent, and all chemical shifts were reported in δ unit downfield from Me_4Si. Crystallographic measurements were recorded using graphite monochromated Mo K_α radiation (λ= 0.71073 Å). The structure has been solved by direct methods and refined by full-matrix least-squares techniques on F2 using SHELXTL [39]. The molecular structure plots were obtained using Platon [40] and mercury [41]. The weighted R-factor wR and goodness of fit S and conventional R-factors R are based on F2 and F respectively [41-44].

Synthesis

The synthetic route is shown in Scheme 1. A 1000 ml flask was charged with 300 g of ice and 150 ml of water and cooled to 0°C in an ice bath; then, it was added by 3.38 g (25 mmol) of 4-Aminoacetophenone and 4.70 g (50 mmol) of hydrochloric acid (d = 1.19 g ml^{-1}), a solution of $NaNO_2$ containing 1.80 g (25 mmol) in 25 ml of water was added in 20 min under electromagnetic stirring solution. After further stirring for 15 min, the solution containing 2.7 ml (25 mmol) was slowly added to resulting solution. The mixture was maintained at pH 7-8 by adding appropriate amount of aqueous sodium acetate. The mixture was stirred at room temperature for 1.5 h. The yellow product (yield 95%) was filtered off, washed with water and dried in vacuum. The solid was dissolved in 30 ml pure acetonitrile (stored in a freezer). Orange plate like crystals, which has a melting point of 148-150 °C, was obtained by slow evaporation of the solvent in a week. Infrared and NMR spectra and CHN analysis, were confirmed the AMT structure; ^{1}H-NMR (300 MHz, DMSO-d_6) δ 7.19–7.93 (8H, m, phenyl protons), 12.71(1H, s, NH), 2.42 (3H, s, methyl), 2.51 (3H, s, acyl). ^{13}C {^{1}H} NMR (300 MHz, DMSO-d_6) δ 17.49, 26.35, 112.85, 113.28, 117.16, 126.64, 127.48, 130.00, 130.28, 130.72, 130.96, 133.10, 145.88, 147.55, 196.16. IR (KBr, ν cm^{-1}): 3217.86 (N-H), 3065.53 (C-H,sp^2), 1432.52-1596.66 (C=C), 2919.01, 2985.36 (methyl), 1169.59 (N-N), 1659.42 (C=O). Elemental Anal. Calc. for $C_{15}H_{15}N_3O$ (253.3 g mol^{-1}): C, 71.13; H, 5.97; N, 16.59. Found: C, 71.11; H, 5.90; N, 16.62%, CCDC No is 1430754.

Computational details

The molecular structure of AMT in grand state is designed preparatory and initial improvement was done on the structure with density function theory and Hartree-Fock methods. Thus, the

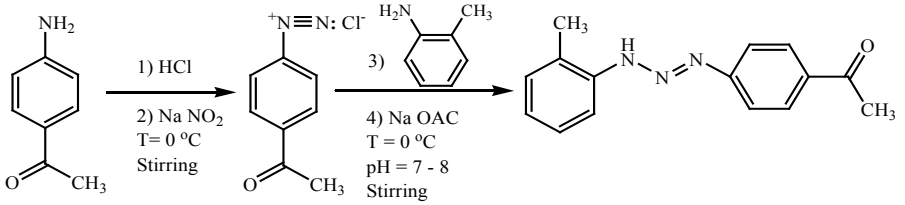

Scheme 1. Synthetic route for the new compound (AMT).

*Gaussian 98w*program package [45], with three different methods HF/B3LYP method with 6-311G (d, p) and B3LYP/6-31G (d) basis sets were used. After the improvement, the vibrational frequency value was calculated and after the calculations, obtained results were extracted and analyzed with *Gauss view 03* software [46]. Vibrational frequencies were exploited with their intensity value and for further consonance of the theoretical vibrational frequencies value with the experimental value was used from scaled factor 0.909 for HF/6-311G (d, p), 0.960 for B3LYP/6-31G (d) method and also 0.967 for B3LYP/6-311G (d, p) method, then started to perform calculations apposite to NMR amounts. For calculation of the NMR amounts GIAO method was used. However, all the chemical shifts were reported based on TMS as a reference [47]. The *VEDA 4* software was used for analysis of the obtained spectra and calculation PEDs percent amounts [48]. All the calculations were done with Pentium IV computer, Intel® CORE™ i7 inside™1.73 GHz job processing with 4 GB of RAMinto Windows^{XP} agent.

Result and Discussion

Description of the crystal structure

AMT structure is obtained during crystallization process in alcoholic environment. This structure is shown in Fig. 1. This structure has orthorombic system with space group, pbca with 8 unit cell molecule that these parameters are comprising of a=8.0665 Å, b=8.0019 Å and c=21.5249 Å (Table 1). In this structure amount of *R*(int) for reflection was 0.0306 (Fig. 2). The molecular formula of this structure is $C_{15}H_{15}N_3O$ and its molecular weight is 253.3. The obtained amounts for some bonds length as N11–C5=1.422 Å, N14–C18=1.391 Å demonstrate approximation the results with the obtained amounts for similar molecules like the DMPF that for C–N bond has 1.4130 Å, 1.2840 Å, 1.3479 Å amounts [49] and in N,N–bis(2,6-dimethylphenyl)-N-oxidoformamidinium compound C–N bond length amount is 1.322 Å [50] also in Benzamideoxime structure amount of C–N bend is 1.350 Å [51]. N11–N12 bond length is 1.262 Å that has double state. In N14–N12 the bond length is 1.332 Å which is simple form. However, for N11–N12–N14 presents an angle approximately 113.2 (˚) and also there are N12 –N11–C5=112.1, N12–N14–C18=119.3 (˚). The most important dihedral angles present in C5–N11–N12–N14=179.9 and C18–N14–N12–N11=179.0 (˚) that are similar to the results of bonding angles in DMPF and Benzamideoxim structures [49, 51]. The AMT structure is able to produce polymer with eight cell unit that is done with very strong hydrogen bond production (Fig 2).

Figure 1 shows the AMT optimal structure with atoms number. This structure recovered by B3LYP method 6-31G (d) and 6-311G (d, p) basis sets, HF method and 6-311G (d, p) basis set. The results were reported in Table 2. The obtained results for the bonds length, bonds angle and also the dihedral angle are similar to experimental results. For example, C5–C9–C13, C26–C29–O30, C2–C5–N11 bonding angle use B3LYP/6-311G (d, p) method respectively is 121.3 (˚), 120.8 (˚) and 123.9 (˚). That completely consonant with structure X-ray results that obtained respectively 121.2 (˚), 120.4 (˚) and 122.4 (˚), of course these results completely consonant with the results of similar compounds as DMFP and N, N–bis(2,6–dimethylphenyl)–N–oxidoformamidinium [49, 50]. The bonds length comparison also demonstrates this order. However, the bond length amount for Carbon–Oxygen bond was obtained 1.212 Å by use of experimental method, 1.191 Å by use of HF method and 1.217 Å by use of DFT method. The obtained results show Carbon–Carbon bond length in Carbonyl group is a little further into rings C–C bond length. Attention to the experimental results, HF and DFT C26–C29 is respectively 1.482 Å, 1.495 Å and 1.493 Å, and for C29–C31 is 1.486 Å, 1.515 Å and 1.520 Å. The considered results of ring bonds length are

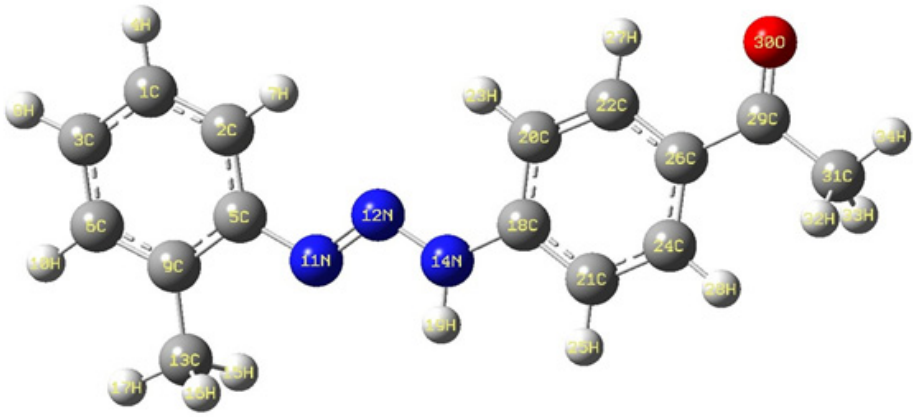

(a)

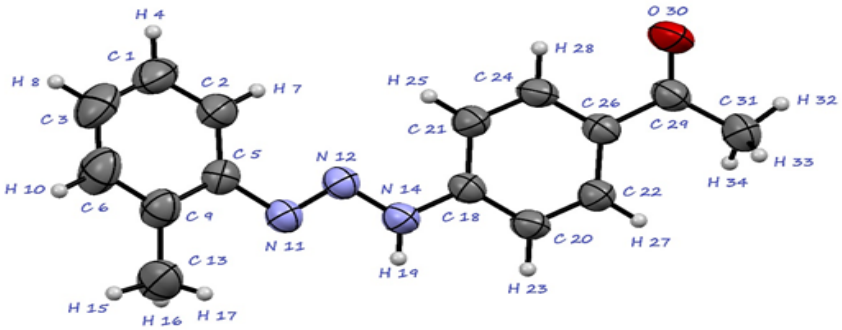

(b)

Fig. 1. (a) Serial number of atom and optimized structure of AMT structure performed byB3LYP/6-311G (d, p) method, (b) The molecular structure of the title compound, displacement ellipsoids are drawn at 50% probability level.

also under effect of mesomery and resonance and adopt closely to each other amounts. The difference of dihedral angles may be ascribed to the intermolecular forces such as Van der Waals interactions and crystal packing forces in the crystal. All of the theoretical calculations were done in gas phase while the experimental calculations are computed in solid phase. But many of the obtained results via the theoretical calculations were close to the experimentally obtained amounts.

Vibrational assignments

The AMT molecule consists of 34 atoms, so it has 96 normal vibrational modes. The observed vibrational assignments and analysis of AMT were discussed in terms of fundamental bands. Table 3 lists the wave numbers of bands observed in FT-IR and FT-Raman spectra (Fig 3) of AMT. The scaled theoretical frequencies and infrared intensities calculated by HF/DFT methods of the AMT were also shown in Table 3. Some bands predicted in FT-IR spectra were not observed in the experimental spectrum of AMT molecule (Fig 4). An overall scaling factor has been applied to the calculated frequencies for these levels. The scaling factors are 0.909, 0.960 and 0.967 for HF/6-31G (d, p), B3LYP/6-31G (d) and B3LYP/6-311G (d, p) respectively. The relativity between calculation and experiments results were studied and the linear function formula was obtained; Y= 0.969X + 15.38 for HF/6-311G (d, p); where R^2 is 0.996, Y= 0.946X + 39.96 for B3LYP/6-31G (d); where R^2 is 0.971, Y= 0.946X + 39.96 for B3LYP/6-31G (d); where R^2 is 0.971, and Y= 0.963X + 35.27 for B3LYP/6-311G (d, p); where R^2 is 0.998 (Fig 5).

C-H vibrations

The C–H vibration type is ranged associated

to molecule structure. Usually C–H stretching vibration in hetro aromatic compounds is observed in frequency range between 2850–3200 cm^{-1}. In N, N–di(p–thiazole)formamidine structure this type of vibration was shown in region 3112, 3113, 3071 and 2978 cm^{-1}, and in 2–chloro–N–(diethylcarbamothioyl) benzamide, structure, C–H stretching was observed in region 2872 cm^{-1} to 3091 cm^{-1} [52], in the AMT structure, three important vibrations 2741, 2919 and 2985 cm^{-1}, duration FT-IR method and four important vibration 2774, 3020, 3060 and 3123 cm^{-1} by FT–Raman method were observed. The obtained results were confirmed use of B3LYP and HF theoretical methods. However, for C-H bending vibrations, there were two in–plane and out–of plane vibrational states. A vibration in range of 1000 cm^{-1} to 1300 cm^{-1} was attended for aromatic in–plane bending vibration. The most important of these bending vibrations were observed use B3LYP/6-311G (d, p) method 1141, 1151, 1162 and 1200 cm^{-1}. Those results were confirmed by PEDs analyses which were close to the AMT results that its in–plane vibrations were 1277, 1253, 1247, 1139 and 1136 cm^{-1}. Intensity of these vibrations was approximately fine and strong. The vibrations 1033, 1030, 1012 and 974 cm^{-1} were seen use of B3LYP/6-311G (d, p) method for C–H out–of plane bending vibration. The C–H bending vibrations 1110, 1078, 1045 and 1021 cm^{-1}, C–H also was recognizable in experimental results that have the week intensity to in–plane vibrations.

C=O and CH_3 vibrations

The C–H bending vibrations were observed on two forms. For aromatic ring C–H that have SP^2 hybridation was seen 3065 and 3040 cm^{-1} use FT-IR method, 3123, 3060 and 3020 cm^{-1} in FT-Raman method. The obtained theoretical results and PEDs analyses have demonstrated this. But the bending C–H for CH_3 was seen in region sub 3000 that 2919 cm^{-1} and 2985 cm^{-1} was seen using the FT-IR and 2774 cm^{-1} in FT-Raman, because the CH_3 hybridation is SP^3 meanwhile for C=O was seen a vibration of 1659 cm^{-1} in FT-IR and 1754 cm^{-1} in FT-Raman, 1780 cm^{-1} in HF method,1699 cm^{-1} in B3LYP/6-31G (d) method and 1693 cm^{-1} in B3LYP/6-311G (d, p) method, that its intensity was very much in FT-IR spectrum. In 2-chloro-N-(diethylcarbamothioyl) benzamide structure was observed use of the FT-IR method vibration amplitude in region 1655 cm^{-1} and use of the B3LYP the vibration amplitude in region 1723 cm^{-1} that were very close with the AMT structure result. But the bending vibrations for C–O was seen also in 588, 559, 496 cm^{-1} in the FT-IR spectrum. Those theoretical vibrations confirm this topic use the B3LYP/6-311G (d, p) method.

C-C vibrations

Carbon–Carbon vibration will different in the various parts of structure. The C–C stretching vibrations are changed in region 1430 to 1625 cm^{-1}. In general, the bands are of variable intensity and are observed at 1625–1590 cm^{-1}, 1590–1575 cm^{-1}, 1540–1470 cm^{-1}, 1465–1430 cm^{-1} and 1380–1280 cm^{-1} from the wave number ranges given by Varsanyi [53] for the five bands in the region. The C=C stretching vibration in the FT-IR spectrum was observed in region 1521, 1586 and 1596 cm^{-1}, in the FT-Raman spectrum was observed in region 1600 cm^{-1}. These results were completely consonance with the theoretical results in the B3LYP/6-311G (d, p) method this vibration was observed in region 1560, 1566, 1587 and 1589 cm^{-1}. The obtained results were similar to the obtained vibrations amplitude for C=C in DMFP and N, N–di(p–thiazole)formamidine [49, 50]. But C–C–C bending vibration was observable in the FT-IR spectrum in region 496, 559, 623, 646 and 696 cm^{-1} that was observed use the theoretical calculations in the B3LYP/6-311G(d, p) level of theory, the bending vibrations in region 525, 551, 599, 619, 639 and 703 cm^{-1}. In DMFP structure the C–C–C vibrations were seen in region 800, 618, 573 and 483 cm^{-1}that are close and similar to obtained results. For the AMT structure [49], of course, it is mention that the intensity of these peaks was at middle region and approximately week. In the Benzamideoxime structure this vibration was seen use experimental methods in region 600 cm^{-1} and 625 cm^{-1} [51]. But the PEDs shows which of vibrations maybe not seen individual at frequency, but closing of the theoretical and the experimental was respectively and detectable.

N-H vibrations

In AMT is presented one hydrogen linked to nitrogen group. In all hetrocyclic compounds N–H stretching vibration is recognizable in region 3000 cm^{-1} to 3500 cm^{-1}. Tsuboi [54] reported the N–H stretching frequency at 3481 cm^{-1} in aniline. However, in DMFP structure the N–H stretching vibration obtained experimentally in region 3301 cm^{-1} and by B3LYP/6-311+G (d, p) method in region 3448 cm^{-1} [49]. In N, N–di(p–thiazole)

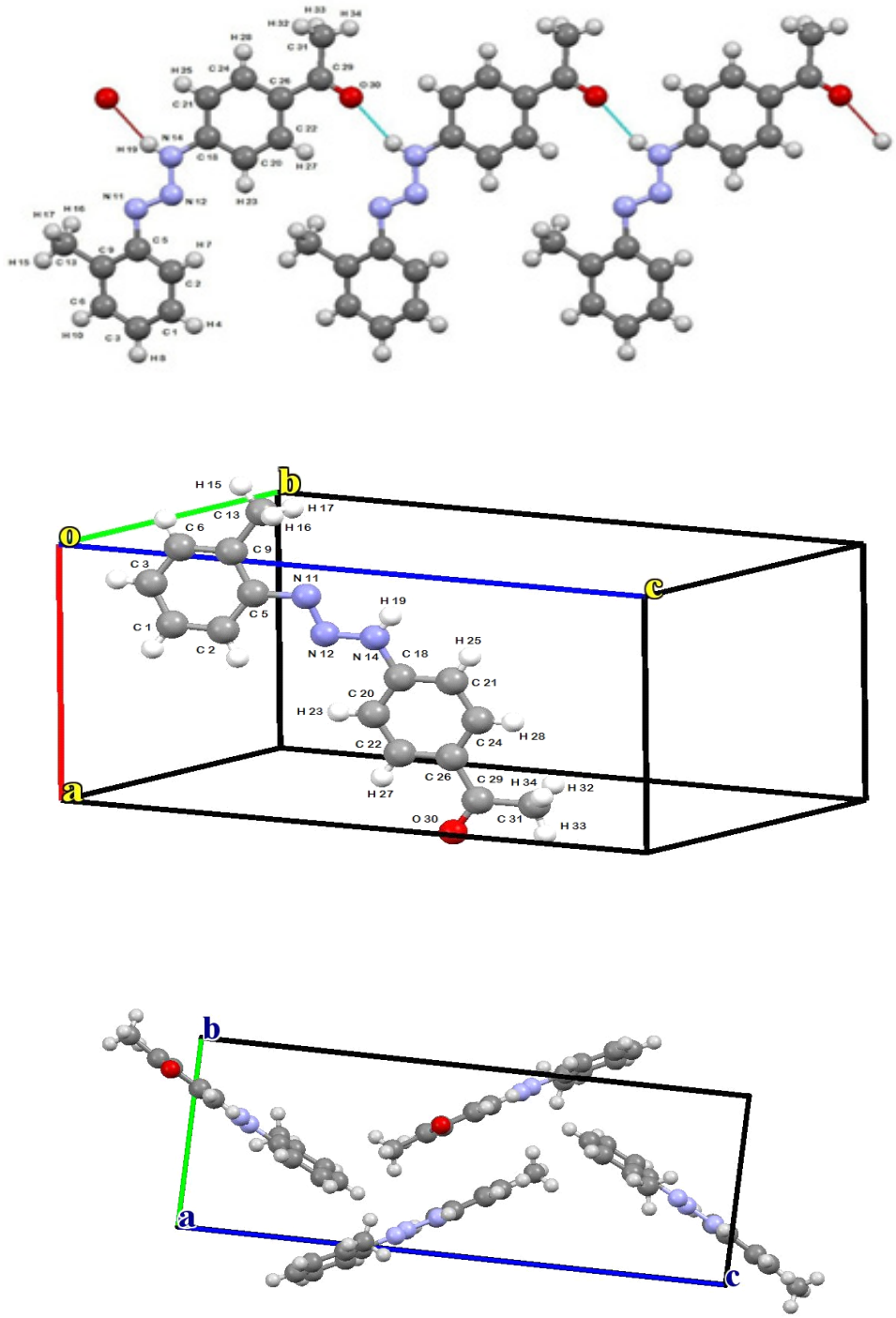

Fig. 2. A view of the crystal packing down the α-axis for the title compound. Hydrogen bonds are shown as dashed lines.

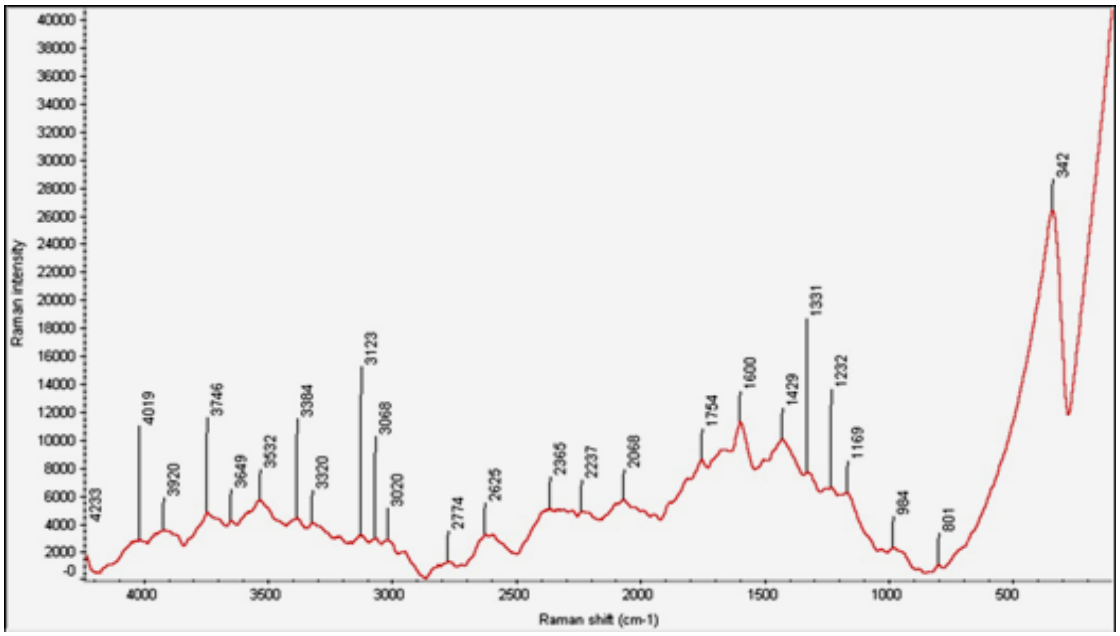

Fig. 3. FT-Raman spectrum of AMT.

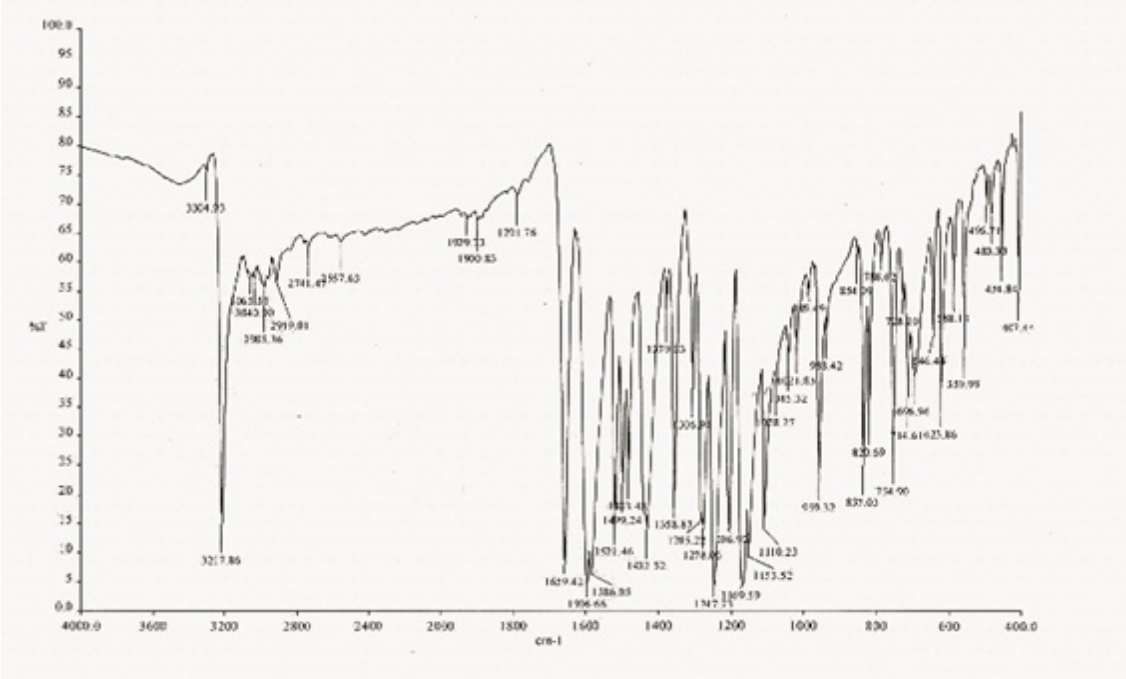

Fig. 4. Show FT-IR spectrum obtained experimental method for the title compound.

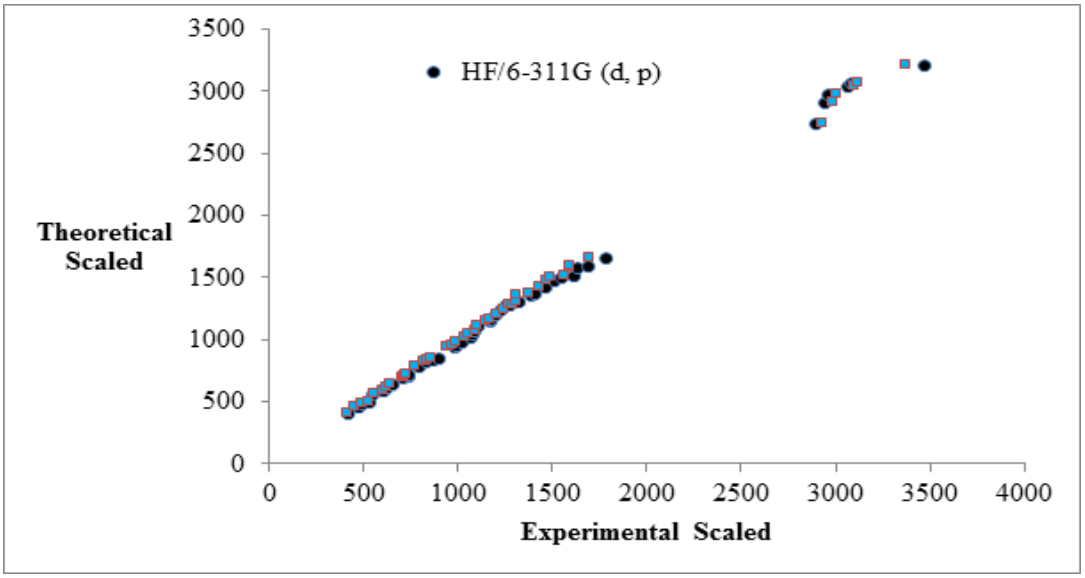

Fig. 5. Correlation between experimental and theoretical frequencies [HF/6-311G (d, p) and B3LYP/6-311G (d, p) methods].

formamidine structure the N–H stretching vibration in region 3258 cm^{-1} was observed [50]. The FT-IR spectrum results showed the value of the N–H stretching vibration in AMT with very strong intensity in region 3217 cm^{-1} and the FT-Raman also shows how this vibration with lighter intensity in region 3532 cm^{-1}. However, the results of HF/6-311G (d, p), B3LYP/6-31G (d) and B3LYP/6-311G (d, p) methods showed the N–H vibration respectively in frequencies 3463, 3344 and 3369 cm^{-1}, for the in–plane bending vibration was observed in regions 1231, 1456 and 1507 cm^{-1} use B3LYP/6-311G (d, p) method. For similar compounds such as N, N–di(*p*–thiazole) formamidine, these vibrations were obtained in region 1278, 1410 and 1545 cm^{-1} and the out–of plane the N–H bending vibration was observed in region 603 cm−1. This vibration was obtained in region 565 cm^{-1} for the structure and N, N–di(p–thiazole) formamidine [50]. In Benzamideoxime structure, the bending N–H vibration same amplitude was observed in region 3233 cm^{-1} and 3262 cm^{-1} that correspond with the obtained results for AMT [51].

C-N vibrations

In aromatic amines C–N range is variable in region 1200 cm^{-1} to 1330 cm^{-1}. In compounds such as benzoxazolethe C–N stretching vibration obtained as 1332 cm^{-1} (FT-IR), 1315 cm^{-1} (FT-Raman) and 1315 cm^{-1} (HF) [55]. However, in the DMFP structure the vibration value was observed by B3LYP method in 1253 cm^{-1} and by FT-Raman method in region 1285 cm^{-1} [49]. In 2–chloro–N–(diethylcarbamothioyl) benzamide structure the C–N vibration amplitude was obtained in region 1221 cm^{-1} and 1203 cm^{-1} that are related to Carbon linked to N–H [52]. For BDMF structure, there are two C–N stretching vibration region. The first vibration is related to Carbon linked to Nitrogen with double bond, which its vibrational amplitude is variable between 1260 cm^{-1} to 1330 cm^{-1} and the second vibration is correlated to Carbon linked to N–H group, that the vibrational amplitude is placed in higher frequency that is demonstrated use PEDs analysis by FT-IR spectrum consideration. The C–N stretching vibration was observed in 1206 cm^{-1}. That it possesses strong peak intensity. The FT-Raman spectrum considers shows the C–N vibration in 1232 cm^{-1}. The theoretical studies in level B3LYP/6-311 G (d, p) demonstrate the experimental results and show the C–N vibration amplitude related to Carbon linked to nitrogen in regions 1200 $cm^{-1}$and 1231 cm^{-1}, related to Carbon linked to N–H in 1537 cm^{-1}. Some bending vibrations of C–N are able to observe with approximately middle intensity using FT-IR method in 407 cm^{-1} and 588 cm^{-1} that correspond completely with theoretical results in B3LYP/6-311G (d, p) level that shows these vibrations in 408 cm^{-1} and 599 cm^{-1}.

N=N and N–N vibrations

In AMT structure N–N bond presents in

TABLE 1. Crystal data and structure refinement.

Empirical formula	**$C_{15}H_{15}N_3O$**
Formula weight	253.3
Temperature (K)	296 (2)
Wavelength (Å)	0.71073
Crystal system, space group	Orthorhombic, *Pbca*
Unit cell dimensions	
a (Å), *α* (°)	8.0665 (2), 90.0000
b (Å), *β* (°)	8.0019 (2), 96.7170 (10)
c (Å), *γ* (°)	21.5249 (5), 90.0000
Volume (Å^3)	1379.84 (6)
Z, Calculated density (Mg/m^3)	4, 1.219
Absorption coefficient (mm^{-1})	0.079
F (000)	536
Crystal size (mm)	0.2× 0.4 × 0.3
Theta range for data collection (deg)	2.61 to 27.00
Max/min. indices *h*, *k*, *l*	-10/10, -10/10, -27/27
Reflections collected	47440
Independent reflections [*R* (int)]	3009 [0.0306]
Completeness to theta = 27.00 (%)	99.80
Refinement method	Full-matrix least-squares on F^2
Data / restraints / parameters	3009/0/181
Goodness-of-fit on F^2	1.057
Final *R* indices [I>2sigma (I)]	R_1 = 0.0431, ωR_2 = 0.1178
R indices (all data)	R_1 = 0.0612, ωR_2 = 0.1366
Largest diff. peak and hole (e.Å^{-3})	0.187 and -0.161

TABLE 2. Computed and experimental bond distances (A), bond angles (◦), torsion angles (◦) for AMT structure.

Parameters	X-ray	HF/6-311G (d, p)	B3LYP/6-31G (d)	B3LYP/6-311G (d, p)
Bond length (Å)				
O30-C29	1.212 (19)	1.191	1.224	1.217
N11-N12	1.262 (16)	1.214	1.263	1.257
N11-C5	1.422 (19)	1.421	1.415	1.414
N14-N12	1.332 (2)	1.328	1.341	1.337
N14-C18	1.391 (2)	1.384	1.389	1.389
C18-C21	1.381 (2)	1.391	1.405	1.402
C18-C20	1.391 (2)	1.395	1.408	1.405
C3-C1	1.364 (3)	1.384	1.398	1.395
C3-C6	1.372 (3)	1.383	1.394	1.392
C1-C2	1.375 (2)	1.381	1.390	1.387
C2-C5	1.391 (2)	1.389	1.405	1.403
C5-C9	1.394 (2)	1.395	1.413	1.410
C20-C22	1.373 (2)	1.376	1.385	1.382
C22-C26	1.387 (2)	1.393	1.407	1.404
C26-C24	1.391 (2)	1.389	1.404	1.401
C26-C29	1.482 (2)	1.495	1.492	1.493
C29-C31	1.486 (2)	1.515	1.522	1.520
C6-C9	1.392 (2)	1.389	1.399	1.397
C9-C13	1.504 (3)	1.511	1.510	1.508
C21-C24	1.374 (2)	1.380	1.389	1.387
Bond Angles (˚)				
N12-N11-C5	112.1 (12)	115.5	115.2	115.6
N12-N14-C18	119.3 (13)	122.2	122.9	112.1
C21-C18-N14	119.5 (13)	118.3	118.4	118.3
C21-C18-C20	119.7 (13)	119.5	119.7	119.6
N14-C18-C20	120.7 (14)	122.3	122.0	122.1
C1-C3-C6	119.9 (18)	119.8	119.8	119.8
C3-C1-C2	120.0 (19)	119.7	119.9	119.8
C1-C2-C5	120.3 (17)	120.3	120.4	120.4
C2-C5-C9	120.1 (15)	120.7	120.3	120.3
C2-C5-N11	123.4 (14)	122.8	124.1	123.9
C9-C5-N11	116.4 (14)	116.4	115.6	115.9
N11-N12-N14	113.2 (12)	113.5	111.7	112.1
C22-C20-C18	119.5 (14)	119.5	119.4	119.5
C20-C22-C26	121.5 (14)	121.8	121.7	121.7
C22-C26-C24	118.0 (13)	118.0	118.2	118.2
C22-C26-C29	119.1 (13)	118.7	118.5	118.5
C24-C26-C29	122.7 (14)	123.3	123.3	123.3
O30-C29-C26	120.4 (15)	120.7	120.8	120.8
O30-C29-C31	119.6 (14)	120.4	120.3	120.4
C26-C29-C31	119.9 (14)	118.9	118.9	118.8
C3-C6-C9	121.7 (18)	121.5	121.6	121.6
C6-C9-C5	117.5 (17)	118.0	118.1	118.1
C6-C9-C13	121.1 (17)	120.6	120.7	120.6
C5-C9-C13	121.2 (15)	121.4	121.2	121.3
C24-C21-C18	120.1 (13)	120.1	120.1	120.1
C21-C24-C26	120.9 (14)	121.2	121.0	121.0
Dihedral Angles(˚)				
N12-N14-C18-C21	178.1 (14)	179.3	179.6	179.1
N12-N14-C18-C20	-1.6 (2)	-0.6	-0.3	-0.9
C6-C3-C1-C2	-1.6 (3)	0.3	0.0	0.1
C3-C1-C2-C5	0.3 (3)	0.3	0.1	0.2
C1-C2-C5-C9	2.3 (3)	-1.1	-0.3	-0.5
C1-C2-C5-N11	-178.5 (16)	-179.1	-179.7	-179.5
N12-N11-C5-C2	11.3 (2)	-23.0	-4.5	-7.8
N12-N11-C5-C9	-169.4 (14)	159.0	176.1	173.1
C5-N11-N12-N14	179.9 (13)	178.5	179.3	178.9
C18-N14-N12-N11	179.0 (14)	177.1	179.6	179.3
C21-C18-C20-C22	-0.1 (2)	-0.2	-0.1	-0.1
N14-C18-C20-C22	179.7 (15)	179.8	179.9	179.8
C18-C20-C22-C26	-0.5 (3)	0.1	0.0	0.1
C20-C22-C26-C24	0.6 (2)	0.0	-0.0	0.0
C20-C22-C26-C29	179.0 (15)	180.0	-180.0	180.0
C22-C26-C29-O30	-2.8 (2)	0.1	0.1	-0.1
C24-C26-C29-O30	175.4 (16)	-179.9	179.9	179.8
C22-C26-C29-C31	177.3 (15)	-179.9	179.9	179.8
C24-C26-C29-C31	-4.4 (2)	0.1	-0.1	-0.2
C1-C3-C6-C9	0.4 (3)	-0.2	-0.1	-0.1
C3-C6-C9-C5	2.1 (3)	-0.6	-0.1	-0.2
C3-C6-C9-C13	-176.2 (2)	179.9	-179.9	-180.0
C2-C5-C9-C6	-3.4 (3)	1.2	0.3	0.5
N11-C5-C9-C6	177.3 (16)	179.3	179.7	179.6
C2-C5-C9-C13	174.8 (18)	179.3	-179.9	-179.8
N11-C5-C9-C13	-4.4 (3)	-1.2	-0.5	-0.7
N14-C18-C21-C24	-179.2 (15)	-179.9	-179.9	-179.8
C20-C18-C21-C24	0.6 (2)	0.1	0.1	0.1
C18-C21-C24-C26	-0.4 (2)	0.1	-0.0	-0.0
C22-C26-C24-C21	-0.2 (2)	-0.1	-0.0	-0.1
C29-C26-C24-C21	178.44 (14)	180.0	180.0	179.9

TABLE 3. Vibrational wavenumbers obtained for AMT structure at B3LYP/6-31G (d), B3LYP/6-311G (d, p) and HF/6-311G (d, p) method [harmonic frequency (cm^{-1}), IRint ($Kmmol^{-1}$)].

Mod nos.	Experimental(cm^{-1})		Theoretical wavenumber (cm^{-1})						PED(%)[c]
	FT-IR	FT-Raman	HF/6-311G (d, p)		B3LYP/6-31G (d)		B3LYP/6-311G (d, p)		
			Scaled	IR_{int}[b]	Scaled	IR_{int}[b]	Scaled	IR_{int}[b]	
1			15	0.56	4	1.04	6	0.96	11ΓNNNC + 70ΓCCNN
2			22	2.68	26	0.90	28	0.90	18ΓNNNC + 45ΓNNCC
3			43	0.89	44	0.73	44	0.73	20δCNN + 20δNNN + 30δNNC + 14δNCC
4			63	1.89	70	1.47	69	1.69	79ΓCCCC
5			79	0.18	78	0.40	78	0.30	17ΓCCCN + 18ΓCCCC + 11ΓCNNN + 16λCCCC
6			118	2.57	108	0.07	107	0.13	29ΓNNNC + 28ΓHCCC + 22ΓHCCC
7			126	0.07	130	0.98	130	0.45	19ΓHCCC + 12CCCN + 13λCCCC
8			138	1.07	137	0.44	140	0.37	10δCNN + 16δCNN + 10δNCC + 12δCCC
9			158	0.01	154	0.15	149	0.15	34ΓHCCC + 34ΓHCCC + 22ΓHCCC
10			173	0.92	178	1.90	178	1.79	13δCCC
11			189	3.88	182	4.31	183	3.64	26ΓNNNC + 18ΓNNCC
12			213	8.62	200	5.17	201	6.38	12ΓCCCC + 15ΓCCCC + 14ΓCNNN + 20λCCCC
13			239	7.48	237	7.65	238	7.73	10δNCC + 23δCCC + 14δCCC
14			279	0.03	275	0.07	276	0.08	25ΓCCCC + 26λCCCC + 12λNCCC
15			316	9.75	314	9.34	316	10.29	32δCCC
16		342vs	336	2.13	320	0.01	323	0.02	14ΓCCCC + 33ΓCNNN
17			390	28.57	386	36.44	388	35.33	15δOCC + 12δNNN
18			412	11.41	403	0.04	406	0.03	10ΓHCCC + 40ΓCCCC + 28ΓCCCC
19	407m		416	0.04	405	7.61	408	7.80	15δCCN + 12δNCC + 13δCCC + 22δCCC
20	457w		464	8.48	450	3.34	453	5.99	10ΓHCCC + 22ΓCCCC + 30λCCCC
21			469	3.07	464	1.23	467	1.61	13δCCC + 11δCCC + 21δCCC
22	483w		488	15.99	484	0.33	486	2.87	13ΓCCCC + 10λOCCC + 41λNCCC
23	496vw		521	64.56	521	0.24	525	0.25	14υCC + 10δOCC + 11δCCC + 19δCCC
24			527	4.28	537	0.40	542	1.30	11ΓHCCC + 21ΓCCCN + 10ΓCCCC + 17ΓCCCC
25	559m		547	15.95	546	10.24	551	9.21	16δOCC + 11δCCC
26			560	5.36	574	0.71	579	2.61	25ΓHCCC + 34λOCCC
27	588w		596	34.19	594	6.32	599	6.77	15υCC + 23δOCC + 10δNNC
28			603	8.60	606	90.80	611	79.39	88ΓHNNN
29	623m		622	30.04	614	34.37	619	35.49	15δCCC + 14δCCC + 12δCCC
30	646m		644	7.81	635	8.64	639	8.16	14δCCC + 11δCCC + 10δCCC
31	696m		706	9.60	700	16.84	703	16.71	13υCC + 12υCC + 18δCCC
32	714m		732	0.44	707	11.42	716	22.31	15ΓHCCC + 15ΓHCCC + 11ΓCCCC + 11ΓCCCC
33	728s		736	16.49	709	0.15	722	0.10	14ΓCCCC + 35ΓCCCC + 14ΓCCCC
34			769	14.36	753	28.88	760	29.60	15ΓHCCC + 15ΓHCCC + 16ΓHCCC+ 21ΓCCCC
35	788vw		788	48.92	769	3.76	772	5.97	16υCC + 24δCCC
36			817	2.89	791	23.03	794	25.44	55ΓHCCC + 23ΓHCCC
37	820m	801vw	828	29.45	812	0.74	816	1.18	20δCCC
38	837s		861	43.45	829	26.85	834	31.98	55ΓHCCC + 18ΓHCCC + 12λNCCC
39	854vw		890	1.78	850	1.00	855	1.69	21ΓHCCC + 24ΓHCCC + 36ΓHCCC
40			925	6.45	911	0.01	918	6.74	15δNNN + 10δCCC
41			943	42.18	912	0.91	923	0.03	24ΓHCCC + 58ΓHCCC
42			971	0.02	917	1.51	924	78.21	30υCC + 13ΓHCCC + 13ΓHCCC
43	938w		979	2.06	927	75.35	935	1.78	28ΓHCCC + 32ΓHCCC + 25ΓHCCC
44	959m		983	12.80	947	0.04	964	0.13	37ΓHCCC + 19ΓHCCC + 19ΓHCCC + 17ΓCCCC

TABLE 3. Cont.

45			996	7.71	960	0.21	974	3.76	10υCC + 10δHCH + 12δCCC + 24ΓHCCC + 20ΓHCCC
46			1010	0.24	977	3.31	975	0.26	23ΓHCCC + 58ΓHCCC
47	989vw	984w	1016	0.19	986	1.16	989	1.03	38δCCC + 24δCCC + 17δCCC
48			1035	5.08	1013	1.75	1012	1.01	13ΓHCCC + 13ΓHCCC + 15ΓHCCC + 27δHCC
49			1043	1.81	1033	3.31	1030	2.62	10δHCH + 11δHCH + 16ΓHCCC + 18ΓHCCC + 25ΓHCCC
50	1021w		1058	1.805	1898	3.62	1033	5.23	14υCC + 10υCC + 11υCC + 11δHCC
51	1045w		1070	0.87	1054	1.51	1054	1.66	17υCC + 10υCC + 10υCC + 11ΓHCCC + 10ΓHCCC
52	1078w		1085	132.09	1094	50.40	1095	61.23	10υCC
53	1110s		1096	6.55	1102	4.03	1100	5.23	10υCC + 10υCC + 21δHCC + 16δHCC
54			1112	3.35	1144	78.29	1141	94.64	10υCC + 25δHCC + 16δHCC + 24δHCC
55	1153s		1162	15.95	1155	456.73	1151	467.08	12υNN + 11δHCC + 11δHCC + 11δHCC + 14δHCC
56	1169vs	1169w	1166	502.23	1164	11.05	1162	45.06	16υNN + 19δHCC
57			1180	15.76	1180	110.30	1180	95.68	23υNN + 21υCC
58	1206s		1197	110.99	1202	1.13	1200	1.01	10υCC + 35υNC + 10δHCC
59		1232w	1217	113.43	1237	755.14	1231	784.33	11υCC + 24υNC + 19δHNN
60	1247vs		1222	238.96	1246	138.80	1241	100.88	29υCC
61	1278s		1252	817.71	1269	28.32	1267	23.45	11υCC + 17δHCC + 30δHCC
62	1285s		1265	3.70	1289	17.73	1287	18.03	18δHCC + 11δHCC + 23δHCC + 20 HCC
63			1291	14.20	1304	6.96	1293	11.63	19υCC + 17υCC + 17υCC + 18υCC
64	1306m		1316	11.77	1312	20.66	1304	13.65	14υCC + 21υCC + 20υCC
65	1358s	1331w	1379	70.08	1353	64.61	1305	81.97	24δHCH + 37δHCH + 23δHCH
66	1379w		1401	0.28	1387	0.70	1372	2.17	26δHCH + 42δHCH + 26δHCH
67			1418	44.14	1406	42.16	1402	39.82	28υCC + 16υCC + 11δHCC + 12δHCC
68			1445	8.88	1426	17.03	1419	8.18	19δHCC + 16δHCC + 10δHCH
69		1429m	1447	2.24	1440	12.12	1423	13.56	17δHCH + 43δHCH + 20δHCH
70	1432s		1455	9.74	1448	9.23	1432	7.50	36δHCH + 41δHCH + 17ΓHCCC
71			1456	6.25	1450	5.23	1433	10.69	40δHCH + 37δHCH + 17ΓHCCC
72			1471	34.59	1451	31.98	1447	69.47	20υNN + 17δHCH
73			1494	22.00	1465	32.58	1456	10.17	16δHNN + 12δHCH
74	1483m		1506	26.43	1474	31.70	1468	30.34	18δHCC + 19δHCC + 10δCCC
75	1499s		1542	195.16	1491	68.47	1488	43.79	37νNN
76			1601	173.63	1511	345.95	1507	404.32	12νNN + 14νNC + 27δHNN
77	1521s		1609	17.46	1563	75.61	1560	67.89	27νCC + 22νCC
78			1622	386.33	1570	14.41	1566	20.96	32νCC + 11δCCC
79	1586vs		1629	208.88	1591	12.10	1587	17.49	15νCC + 12νCC + 22νCC + 19νCC
80	1596vs	1600m	1687	252.33	1595	473.91	1589	463.68	30νCC + 10νCC + 11νCC
81	1659vs	1754w	1780	309.67	1699	191.59	1693	204.88	86νOC
82	2741vw	2060w	2887	5.07	2930	3.25	2932	3.34	43νCH + 43νCH + 14νCH
83		2237vw	2888	33.26	2933	28.24	2935	28.59	40νCH + 31νCH + 28νCH
84		2365vw	2939	26.66	2986	11.16	2986	15.72	51νCH + 47νCH
85	2919vw	2625w	2941	18.87	2987	15.55	2988	11.08	50νCH + 50νCH
86	2985w	2774vw	2953	33.57	3004	23.56	3005	24.64	22νCH + 70νCH
87		3020vw	2987	22.76	3042	16.6	3040	17.19	86νCH
88			3016	4.19	3052	11.77	3055	10.09	28νCH + 63νCH
89		3060vw	3020	16.27	3055	11.93	3058	11.33	91νCH
90			3028	20.68	3063	16.47	3066	14.93	60νCH + 11νCH + 26νCH
91			3042	37.33	3078	40.49	3080	32.93	25νCH + 60CH + 10 CH
92			3050	13.58	3083	14.30	3086	10.66	91νCH
93		3123vw	3060	0.42	3094	0.15	3091	0.10	92νCH
94	3040vw	3320vw	3062	5.45	3099	4.98	3100	4.33	92νCH
95	3065vs	3384vw	3078	3.91	3114	3.02	3114	2.29	92νCH
96	3217vw	3532w	3463	36.15	3344	9.79	3369	10.77	100νNH

[a] w-weak; vw-very weak

[b] IRint-IR intensity.

[c] Potential energy distribution (PED) calculated B3LYP/6-311G (d, p). ν stretching, δ: bending, Γ: torsion , λ : out , PED less than 10% are not shown.

TABLE 4. Theoretical and experimental ^{1}H and ^{13}C isotropic chemical shifts (with respect to TMS, all values in ppm) for AMT structure.

	Atomic Number	Methods			
		HF 6311G (d, p)	B3LYP 6-31G (d)	B3LYP 6-311G (d, p)	Exp
Chemical Shift	H19	8.57	8.24	8.84	12.71
	H27	9.00	8.24	8.53	7.93
	H23	7.98	7.69	8.04	7.50
	H7	8.00	7.65	8.02	7.48
	H28	8.16	7.55	7.81	7.42
	H4	7.55	7.09	7.38	7.39
	H10	7.61	7.06	7.41	7.28
	H8	7.58	7.03	7.32	7.25
	H25	6.74	6.32	6.69	7.23
	H16	2.97	2.69	2.90	3.33
	H15	2.53	2.56	2.69	2.52
	H33	2.43	2.44	2.58	2.51
	H32	2.43	2.43	2.57	2.49
	H34	2.21	1.84	2.01	2.48
	H17	2.10	1.72	1.94	2.42
	C29	191.47	184.14	196.24	196.16
	C5	150.81	139.57	153.33	147.55
	C18	155.54	136.12	150.83	145.88
	C9	142.54	130.90	144.46	133.10
	C22	143.47	125.87	137.47	130.96
	C6	136.03	124.75	136.71	130.72
	C24	141.16	124.06	136.01	130.28
	C26	131.27	123.94	136.71	130.00
	C3	135.41	122.00	134.70	127.48
	C1	131.88	120.02	132.18	126.44
	C2	123.23	109.98	120.45	117.12
	C20	113.64	106.55	117.28	113.28
	C21	112.01	106.29	116.73	112.85
	C31	26.73	25.75	28.29	26.35
	C13	20.14	20.64	22.26	17.49

TABLE 5. Correlation between theoretical and experimental methods for NMR property in AMT structure.

Correlation between		Kind of NMR	Equation	R^2
Experimental	HF/6-311G (d, p)	^{13}C-NMR	Y = 1.009X + 3.491	0.988
		^{1}H-NMR	Y = 0.850X + 0.736	0.848
	B3LYP/6-31G (d)	^{13}C-NMR	Y = 0.927X + 2.953	0.988
		^{1}H-NMR	Y = 0.808X + 0.630	0.858
	B3LYP/6-311G (d, p)	^{13}C-NMR	Y = 1.004X + 4.613	0.996
		^{1}H-NMR	Y = 0.845X + 0.689	0.875

two forms simple and doublet, and it causes to have a different vibration in this region. The FT-IR consideration shows how N–N stretching vibration will be very much in 1153 cm^{-1} and 1169 cm^{-1} that correspond with obtained amounts by theoretical calculations in level B3LYP/6-311G (d, p) that shows this vibration amplitude in 1151, 1167 and 1180 cm^{-1}. However for N=N stretching vibration was observed in the FT-IR spectrum in 1499 cm^{-1} with middle intensity. The theoretical calculation in level of B3LYP/6-311G (d, p) theoretical results showed the same amplitude of this vibration in region 1447 cm^{-1} and 1448 cm^{-1}. However, the bending vibration for N–N=N is observed in (PEDs 15%) 918 frequency use B3LYP/6-311G (d, p) method.

NMR spectra

The obtained results for chemical shift, ^{13}C-NMR and ^{1}H-NMR amounts were reported in Table 4. The obtained amounts calculated theoretically using GIAO method, and these calculations were spotted in three theoretical levels B3LYP/6-311G (d, p), B3LYP/6-31G (d) and HF/6-311G (d, p). TMS was spotted as a reference for the obtained results and be closer to the experimental amounts. Thus, the TMS chemical shift amounts were calculated individually using the above methods and were obtained the results for the AMT structure based on that. After the calculation, compared the theoretical and experimental amounts, and obtained a diagram for each method. Linear equation amounts reported in Table 5. But noteworthy point in this spectrum is H19 peak indication in region 12.7 ppm for the experimental spectrum. That by perform HF/6-311G (d, p), B3LYP/6-31G (d) and B3LYP/6-311G (d, p) theoretical methods the amount of chemical shift was obtained respectively in region 8.57, 8.24 and 8.84 ppm. However, for formamidines the chemical shift amounts indicated in region 7 to 8 ppm for this type of hydrogen [49, 50]. But for compounds with three adenine groups the different experimental results showed that due to difference of chemical environment of this hydrogen, the chemical shift is appeared in lower region or be deshield (Fig 6 and 7). To explain this discrepancy, is stated that such theory calculations and other NMR results were performed in gas phase, while the experimental calculations were done in solution phase. It represents that the chemical shift amounts are under effect of solvent experimentally.

Molecular electronic potential maps

First, the AMT structure was optimized by

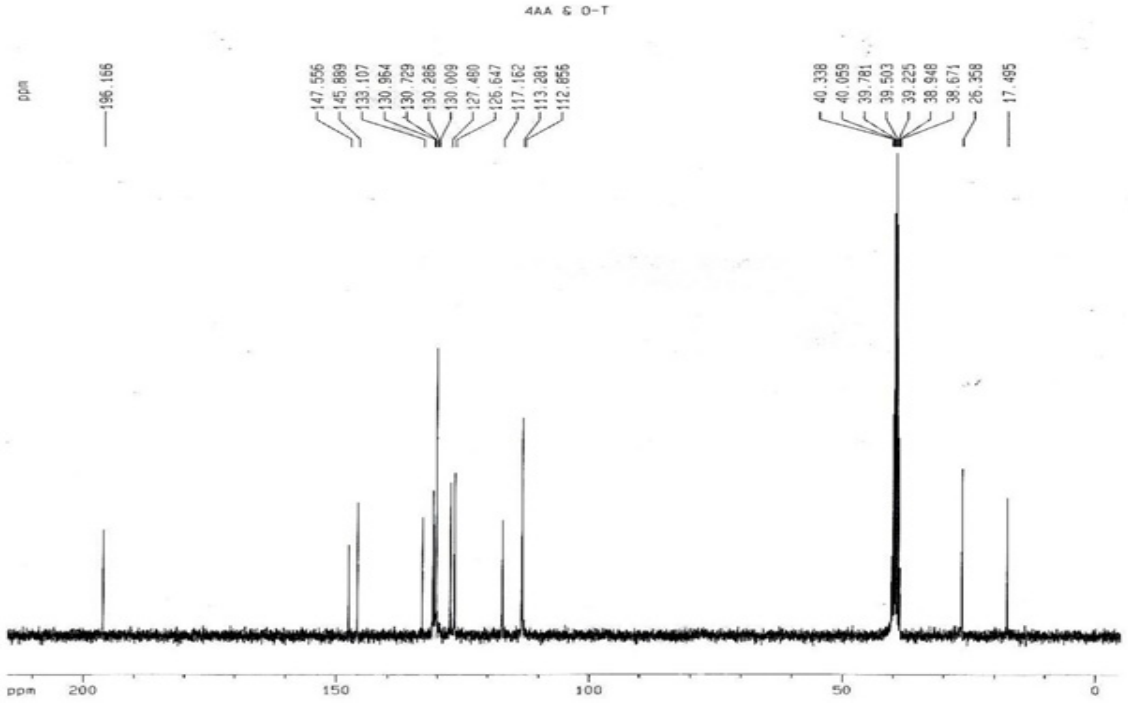

Fig. 6. Show and comparison 13C-NMR spectrum obtained by experimental methods for the title compound.

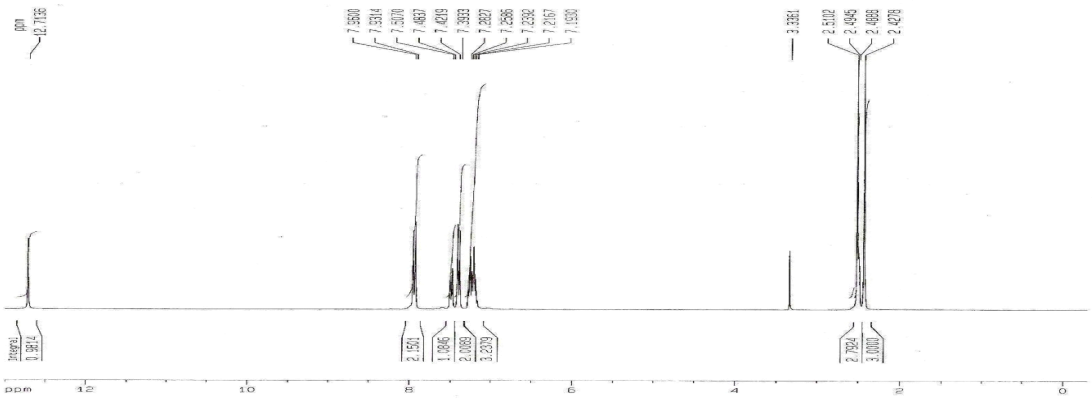

Fig. 7. Show and comparison ^{1}H-NMR spectrum obtained by experimental methods for the title compound.

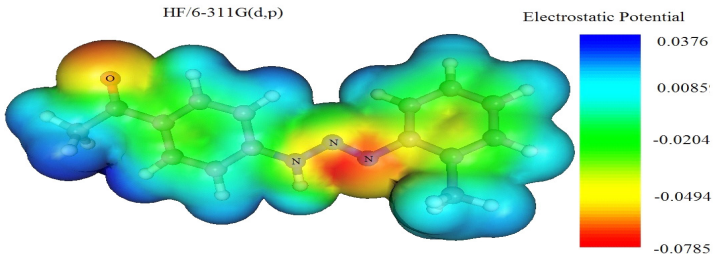

(a)

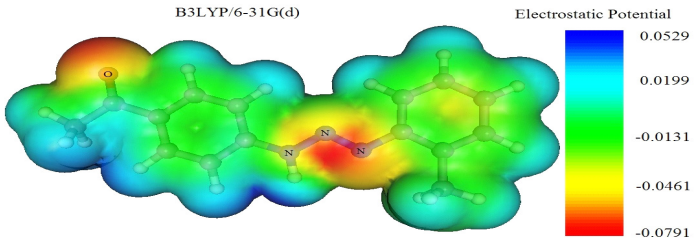

(b)

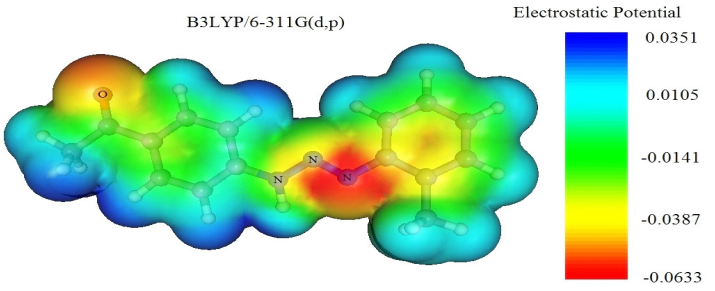

(c)

Fig. 8. (a) HF/6-311G (d, p), (b) B3LYP/6-31G (d) and (c) B3LYP/6-311G (d, p) calculated 3D molecular electrostatic potential of ATM (isosurface value 0.01 a.u.).

B3LYP/6-311G (d, p) method for calculated electronic potential amounts, then calculated the electronic potential amounts in structure [56-60]. Molecular electronic potential maps (MEPM) in fact determine conditions that present the most electrophilic attack probability to these points and they are reactivity value detector of various parts of molecule. As Fig. 8 shows, the electronic potential value is increased by going to blue color, and it decreased by going to red color. The electronic potential value had a negative amount in apart that Oxygen exist, in areas that present also Carbonic groups, the electronic potential is closed to positive amounts namely the blue color.

Other molecular properties

The thermo dynamical parameters, dipole moment and other energetic parameters were reported in Table 6. For this purpose, three methods HF/6-311G (d, p), B3LYP/6-31G (d) and B3LYP/6-311G (d, p) were used. All parameters were calculated in gas phase and the temperature of 298.15 kelvin degrees, and the pressure of one atmosphere, also the calculation of some associated to HOMO and LUMO levels parameters such as chemical hardness (η), chemical potential (μ), electrophilicity (ω) and max amount of electronic charge transfer (ΔN_{max}) was gestured in this table.

Conclusions

First, the AMT structure was synthesized by assigned crystallography method in laboratory and for its recognition, was used ^{1}H-NMR, ^{13}C-NMR, FT-IR, FT-Raman and X-ray single crystal diffraction methods, then considered the thermodynamically parameters, chemical shift value and also the vibrational frequencies using HF/DFT theoretical methods with 6-311G (d, p) and 6-31G (d) basis sets, thus the structure was improved, then calculated the parameters. Three scaled factor of transfer coefficient 0.909, 0.960 and 0.967 were used for three methods HF/6-311G (d, p), B3LYP/6-31G (d) and B3LYP/6-311G (d, p) for more corresponding of the theoretical and experimental obtained results. However, the vibrational spectra were analyzed using *VEDA 4* software and the value of Potential energy distributions was considered, then the theoretical and experimental results were compared, the obtained results showed the theoretical amounts were closed to experimental results and they correspond to each other completely. The theoretical method B3LYP/6-311G (d, p) showed the most corresponding with the obtained experimental results, from three performed theoretical methods.

TABLE 6. Theoretically computed energies (kcal.mol−1), zero-point vibrational energies (kcal.mol−1), rotational constants (GHz), heat capacities (cal.mol-1.K-1), entropies (cal.mol-1.K-1), dipole moment (Debye), molecular orbitals energies (εHOMO and εLUMO, eV), electronic chemical potential, μ (eV), chemical hardness, h (eV), electrophilicity, ω (eV) and maximum amount of electronic charge transfer for AMT structure.

Parameters	HF/6-311G(d, p)	B3LYP/6-31G(d)	B3LYP/6-311G(d, p)
Total energy	-511303.316	-514430.903	-514561.463
ZPVE	182.25362	171.54501	170.34596
Rotational constant	1.26256	1.28386	1.28610
	0.12369	0.12073	0.12099
	0.11384	0.11054	0.11086
Entropy			
Total	134.848	140.669	140.100
Translational	42.487	42.487	42.487
Rotational	34.158	34.194	34.188
Vibrational	58.204	63.988	63.426
Heat capacity	61.675	65.739	65.940
Dipole moment(D)	3.9404	3.7862	3.7994
HOMO	-0.29470	-0.20884	-0.21813
LUMO	0.07248	-0.07194	-0.08090
Chemical potential(μ)	-0.11111	-0.14039	-0.14951
Chemical hardness(η)	0.36718	0.13690	0.13723
Electrophilicity(ω)	0.01681	0.07198	0.08144
ΔN_{max}	0.30260	1.02549	1.08952

Acknowledgements

The authors are indebted to Ms Esfandiar for his interest in this work and many helpful discussions. However, this work was supported by Islamic Azad University, Shahre-rey Branch.

References

1. Ang H. G., Koh L. L., Yang G. Y., *J. Chem. Soc., Dalton Trans.* 1573 (1996).

2. Rouzer C. A., Sabourin M., Skinner T. L., Thompson E. J., Wood T. O., Chmurny G. N., Klose J. R., Roman J. M., Smith Jr. R. H., Michejda C., *J. Chem. Res. Toxicol,* **9,** 172 (1996).

3. Nicolau K. C., Boddy C. N. C., Li H. , Koumbis A. E., Hughes R., Natarajan S., Jain N. F., Ramanjulu J. M., Bra¨se S., Soloman M., *Chem. Eur. J,* **5,** 2602 (1999).

4. Jones L., Schumm J. S., Tour J. M., *J. Org. Chem,* **62,** 1388 (1997).

5. Jian H., Tour J. M., *J. Org. Chem,* **70,** 3396 (2005).

6. Lippert T. , Nuyken O. , *Makromol. Chem., Rapid Commun,* **13,** 365 (1993).

7. Wanner M. J., Koch M., Koomen G. J., *J. Med. Chem,* **47,** 6875 (2004).

8. Monica Barra N.C., Lee I., Chahal N., *J. Org. Chem,* **67** 2271 (2002).

9. Buruiaba E., Melinte V., Buruiana T., Simionescu B., Lippert T., Urech L., *J.Photo. Chem.* **44,** 5271 (2006).

10. Safavi A., Haghihi B., Frescnius J., *J. Anal. Chem.* **357,** 870 (1997).

11. Rofouei M.K., Aghaei A., *J. Iran. Chem. Soc.* **10**,969 (2013).

12. Gholivand M.B., Mohammadi M., Khodadadian M., Rofouei M.K., *Talanta* **78** 922 (2009).

13. Gholivand M.B., Mohammadi M., Rofouei M.K., *Mater. Sci. Eng.* **C 30,** 847 (2010).

14. Rofouei M.K., Payehghadr M., Shamsipur M., Ahmadalinezhad A., *J. Hazard. Mater.* **168,** 1184 (2009).

15. Rofouei M.K., Sabouri A., Ahmadalinezhad A., Ferdowsi H., *J. Hazard. Mater.* **192,** 1358 (2011).

16. Hill D.T., Stanley K.G., Williams J.E., Love B., P.J. Fowler, McCafferty J.P., Macko E., Berkoff C.E., Ladd C.B., *J. Med. Chem.* **26,** 865 (1983).

17. Brahimi F., Rachid Z., McNamee J.P., Alaoui-Jamali M.A., Tari A.M., Jean-Claude B.J., *Biochem. Pharmacol.* **70,** 511 (2005).

18. Jean-Claude B.J., Mustafa A., Damian Z., De Marte J., Vasilescu D.E., Yen R., Chan T.H., Leyland Jones B., *Biochem. Pharmacol.* **57** 753 (1999).

19. Friedman H.S., Kerby T., Calvert H., *Clin. Cancer Res.* **6,** 2585 (2000).

20. Agarwala S.S., Kirkwood J.M., *Oncologist* **5,** 144 (2000).

21. Nicolaou K.C., Boddy C.N.C., Li H. , Koumbis A.E., Hughes R., Natarajan S., Jain N.F., Ramanjulu J.M., Bräse S., Solomon M.E., *Chem. Eur. J.* **5,** 2602 (1999).

22. Lazny P., Sienkiewicz M., Brase S., *Tetrahedron* **57,** 5825 (2001).

23. Knochel P., Liu C.Y., *Org. Lett.* **7,** 2543 (2005).

24. Kimball D.B., Weakley T.J.R., Herges R., Haley M.M., *J. Am. Chem. Soc.* **124,** 13463 (2002).

25. Dabbagh H.A., Teimouri A., NajafiCh A., Shiasi R., *Spectro. Chim.ActaPart A.* **67,** 437 (2007).

26. Boeringer Sohn C.H. , *German Offen.* **2,** 301 (1974).

27. Eleventh Report on Carcinogens (2004).

28. Rofouei M.K., Soleymani R., Aghaei A., Mirzaei M., *Journal of Molecular Structure,* **1125,** 247 (2016).

29. Immirzi A., Porzio W., Bombieri G., Toniolo L., *J. Chem. Soc. Dalton Trans.*1098 (1980).

30. Melardi M.R., Rofouei M.K., Massomi J., *Anal. Sci.* **23,** x67 (2007).

31. Bourissou D., Guerret O., Gabbaı F. P., Bertrand G., *Chem. Rev,* **100,** 39 (2000).

32. Horner M., de Oliveira G. M., Bresolin L., de Oliveira A. B., *Inorg. Chim.Acta.***359,** 4631 (2006).

33. Marchesi F., Turriziani M., Tortorelli G., Avvisati G., Torino F., DeVecchis L., *Pharmacological Research.* **56,** 275 (2007).

34. Lehn J.M., *Science*. **260,** 1762 (1993).

35. Stupp S.I., Lebonheur V., Walker K., Li L.S., Hugging K.E., Kesser M., Amstutz A., *Science*. **276,** 276 (1997).

36. Dalgarno S.J., Power N.P., Atwood J.L., *Coord. Chem..Rev.* **252,** 825 (2008).

37. Parr R.G., Szentpaly L.V., Liu S., *J. Am. Chem. Soc.* **121,** 1922 (1999).

38. Chamorro E., Duque-Norea M., Perez P., *J. Mol. Struct*. **896,** 73 (2009).

39. Sheldrick G. M., *ActaCryst., A.* **64,**112 (2008).

40. Spek A.L., PLATON, A Multipurpose Crystallographic Tool, Utrecht University, Utrecht, Netherlands (2005).

41. Mercury 1.4.1, Copyright Cambridge Crystallographic Data Centre, 12 Union Road.

42. Ganjali M.R., Rouhollahi A., Mardan A.R., Shamsipur M., *J. Chem. Soc., Faraday Trans.* **94,** 1959 (1998).

43. Fakhari A., Shamsipur M., *J. Inclusion Phenom.* **26,** 243 (1996).

44. D. M. Khramov, C. W. Bielawski, J. Org. Chem. *72* (2007) 9407.

45. Frisch M.J., Trucks G.W., Schlegel H.B., Scuseria G.E., Robb M.A., Cheeseman J.R., Montgomery J.A., Vreven T., Kudin K.N., Burant J.C., Millam J.M., Iyengar S.S., Tomasi J., Barone V., Mennucci B., Cossi M., Scalmani G., Rega N., Petersson G.A., Nakatsuji H., Hada M., Ehara M., Toyota K., Fukuda R., Hasegawa J., Ishida M., Nakajima T., Honda Y., Kitao O., Nakai H., Klene M., Li X., Knox J.E., Hratchian H.P., Cross J.B., Adamo C., Jaramillo J., Gomperts R., Stratmann R.E., Yazyev O., Austin A.J., Cammi R., Pomelli C., Ochter ski J.W., Ayala P.Y., Morokuma K., Voth G.A., Salvador P., Dannenberg J.J., Zakrzewski V.G., Dapprich S., Daniels A.D., Strain M.C., Farkas O., Malick D.K., Rabuck A.D., Raghavachari K., Foresman J.B., Ortiz J.V., Cui Q., Baboul A.G., Clifford S., Cioslowski J., Stefanov B.B., Liu G., Liashenko A., Piskorz P., Komaromi I. , Martin R.L., Fox D.J., Keith T. , Al-Laham M.A., Peng C.Y., Nanayakkara A., Challacombe M., Gill P.M.W., Johnson B., Chen W., Wong M.W., Gonzalez C., Pople J.A , Gaussian 03 Revision C.02, Gaussian Inc.,Pittsburgh, PA, (1998).

46. Dennington R., Keith T., Millam J., Eppinnett K., Lee Hovell W., Gilliland R.,*Gauss View,* Version 3. 07, Semichem, Inc., Shawnee Mission, KS, (2003).

47. Wolinski K., Hinton J.F., Pulay P., *J. Am. Chem. Soc.* **112,** 8251 (1990).

48. Jamroz M.H, Vibrational Energy Distribution Analysis VEDA 4, Warsaw, (2004).

49. Rofouei M.K., Sohrabi N., Shamsipur M., Fereyduni E., Ayyappan S., Sundaraganesan N., *Spectrochimica Acta Part A.* **76,** 182 (2010).

50. Rofouei M.K., Fereyduni E., Sohrabi N., Shamsipur M., Attar Gharamaleki J., Sundaraganesan N., *Spectrochimica Acta Part A.* **78,** 88 (2011).

51. Arjunan V., Mythili C.V., Mageswari K., Mohanc S., *Spectrochimica Acta Part A.* **79,** 245 (2011).

52. Hakan Arslan, Ulrich Fl¨orke, Nevzat K¨ulc¨u, G¨un Binzet, *SpectrochimicaActa Part A*. **68,** 1347 (2007).

53. Shimanouchi T., Kakiuti Y., Gamo I., *J. Chem. Phys.* **25,** 1245 (1956).

54. Tsuboi M., *Spectrochim. Acta A.* **16,** 507 (1960).

55. Saxena R., Kauedpal L.D., Mathur G.N., *J. Polym. Sci. A: Polym. Chem.* **40,** 3559 (2002).

56. Politzer P., Truhlar D.G. (Eds.), *Chemical Application of Atomic and Molecular Electrostatic Potentials,* Plenum, New York, (1981).

57. Soleymani R., Mohammad Salehi Y., Yousofzad T., Karimi-Cheshmeh Ali M., *Oriental Journal of Chemistry* **28,** 627 (2012).

85. Soleymani R., Dijvejin R.D., Hesar A.F.G.A., Sobhanie E., *Oriental Journal of Chemistry,* **28,** 1291 (2012).

59. Soleymani R., Dijvejin R.D., Hesar A.F.G.A., *Oriental Journal of Chemistry,* **28,** 1107 (2012).

60. Zarei G., Soleymani R., Dejvejen R. D., *Oriental Journal of Chemistry,* **28,** 1229 (2012).

(*Received* 27/11/2017;
accepted 22/ 2 /2018)